

# Estimation Model of Spacecraft Parameters and Cost Based on a Statistical Analysis of COMPASS Designs

Matthew W. Gerberich<sup>1</sup> and Steven R. Oleson<sup>2</sup>  
*NASA Glenn Research Center, Cleveland, OH 44135*

The Collaborative Modeling for Parametric Assessment of Space Systems (COMPASS) team at Glenn Research Center has performed integrated system analysis of conceptual spacecraft mission designs since 2006 using a multidisciplinary concurrent engineering process. The set of completed designs was archived in a database, to allow for the study of relationships between design parameters. Although COMPASS uses a parametric spacecraft costing model, this research investigated the possibility of using a top-down approach to rapidly estimate the overall vehicle costs. This paper presents the relationships between significant design variables, including breakdowns of dry mass, wet mass, and cost. It also develops a model for a broad estimate of these parameters through basic mission characteristics, including the target location distance, the payload mass, the duration, the delta-v requirement, and the type of mission, propulsion, and electrical power. Finally, this paper examines the accuracy of this model in regards to past COMPASS designs, with an assessment of outlying spacecraft, and compares the results to historical data of completed NASA missions.

## Nomenclature

$M_D$	=	dry mass, kg
$M_{PL}$	=	payload mass, kg
$M_f$	=	final mass, kg
$M_o$	=	initial mass, kg
$M_{PP}$	=	propellant mass, kg
$g_0$	=	acceleration due to Earth's gravity, m/s <sup>2</sup>
$I_{sp}$	=	specific impulse, s
$\Delta V$	=	change in orbital velocity, m/s
$EP$	=	electric propulsion
$SEP$	=	solar electric propulsion
$REP$	=	radioisotope electric propulsion
$GN\&C$	=	guidance, navigation, and control
$C\&DH$	=	command and data handling

## I. Introduction

IN 2006, NASA's Glenn Research Center created the Collaborative Modeling for Parametric Assessment of Space Systems (COMPASS) team, in order to perform analysis and design assessments of new spacecraft.<sup>7</sup> Since being established, the team has completed over 90 mission designs as of the writing of this report, covering a variety of vehicle types and objectives, including an asteroid retrieval feasibility study.<sup>11</sup> COMPASS proceeds by performing iterative and concurrent analyses of each spacecraft subsystem, consisting of the guidance, avionics, communications, power, thermal, structures, and propulsion systems. The subsystems are cataloged in a mass equipment list (MEL), detailing the mass of each individual component. Once the overall system design has been established, a parametric cost estimation follows using cost estimation relationships (CERs), assigning a price to each component based on historical data, mass, and technological readiness levels. These estimates are designed to

<sup>1</sup> Summer Intern, Mission Design and Analysis Branch, from Purdue University, AIAA Student Member.

<sup>2</sup> COMPASS Lead Engineer, Mission Design and Analysis Branch, MS 142-6, AIAA Senior Member.

account for the design, development, testing, and manufacturing expenses that go into the spacecraft's cost, as well as launch costs, mission operation costs, and margins built in to account for growth as the project progresses.<sup>3</sup>

Although this method is effective, it is also useful to have broad estimates of the spacecraft parameters before designing begins. Initially, the COMPASS team knows the objective of the mission and the mass of the payload. In the majority of spacecraft, this payload is the scientific instrumentation, while in some communications satellites, such as the Lunar Relay Satellite design<sup>8</sup>, communicative devices are considered to be the payload, rather than treated as a separate subsystem (in this case, that subsystem mass is listed as zero kilograms). In rockets and rocket stage missions, such as the Earth Departure Stage design, the payload is the entire mass which is going to be delivered to a new orbit or trajectory. Via various mass relationships, the payload mass can be used to estimate the spacecraft dry mass, which is the overall mass excluding the propellant, and the bus mass, which is the dry mass excluding the payload. Typically, these two mass definitions exclude passive or protective equipment, such as aeroshells. Furthermore, averages of mass breakdowns for different spacecraft types can be used to estimate each subsystem mass. Historically, some mass relationships have been explored by Larson and Wertz<sup>3</sup>, and Brown<sup>5</sup>, among others.

In addition to the payload mass, the team completes a mission architecture and trajectory analysis prior to the actual design study, which establishes mission details including the launch vehicle, launch date, and overall required  $\Delta V$ , or orbital velocity changes.<sup>7</sup> Typically, the type of power and propulsion systems to be used on the spacecraft will be known as well, or will be traded on during the study to reduce mass and cost. This information can then be used to determine the mass of the necessary propellant, and by doing so, the overall spacecraft mass.

Once mass values have been estimated, CERs can be used to result in order-of-magnitude estimations of the final spacecraft costs. However, rather than the equipment-level costing typically done at the completion of COMPASS studies, broad estimates may use system-level relationships, based on bus mass, dry mass, or wet mass, as well as subsystem costs per mass. CERs for overall spacecraft parameters can be found in *Space Mission Analysis and Design*<sup>3</sup>, however, the types of spacecraft used for historical data were typically low-Earth orbit satellites. We hope that an examination completed based on past COMPASS designs should offer a broader variety of design types, and should be more suited to the low technological readiness level of the equipment used in many forward-looking design studies typically completed by the team.

## II. Dry Mass

Eleven COMPASS missions were piloted spacecraft; as these were usually an order of magnitude or two larger than other missions, we frequently could not compare them along with other missions. Of the remaining unmanned

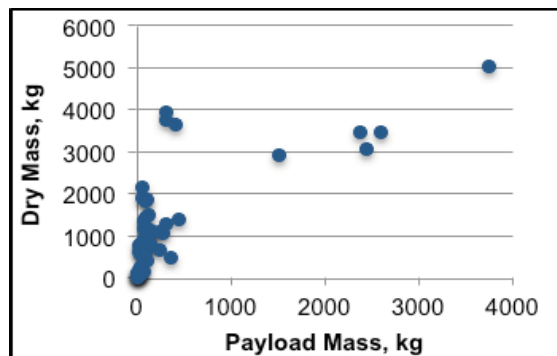


Figure 1. Dry Mass versus Payload Mass.

missions, mass data was available for fifty-five spacecraft. Fig. 1 presents all of these past designs' dry mass versus payload mass; as can be seen, there seems to be no direct correlation between the variables. However, this figure includes dissimilar missions that should not be compared directly; instead, these 55 vehicles can be broken into several classifications. One such classification is interplanetary spacecraft, which perform science or communications work during flyby, rendezvous, or sample-return trajectories to other planets or solar system bodies; there are 20 such vehicles. The 12 vehicles which complete science or communications missions, but do not leave Earth's gravitational sphere of influence (including those in lunar orbit) make up another category. These two

categories, along with a group of transfer vehicles and spacecraft rocket stages (containing seven mission designs), as well as landers on the Moon, Mars, and Venus (also consisting of seven mission designs), comprise the traditional unmanned spacecraft that COMPASS has designed. In addition to the primary spacecraft, they have completed system analyses on three rovers, two gas-balloon suspended gondolas, and four trades on the Mars Ascent Vehicle, which would have been part of a larger sample return architecture<sup>10</sup>, as well as a dual payload attachment fitting.

Because of the dissimilar nature of the non-spacecraft missions, and the small number of comparable cases, it was not possible to explore their relationships between payload mass and dry mass. For the other spacecraft, the vehicle dry mass was plotted against payload mass, as shown in Fig. 2 for the Earth and lunar missions, Fig. 3 for the interplanetary missions, Fig. 4 for landing craft, and Fig. 5 for stage vehicles. Each graph demonstrates a clear linear fit pattern, which has been shown on each graph using Microsoft Excel's trendline tool on all data points.

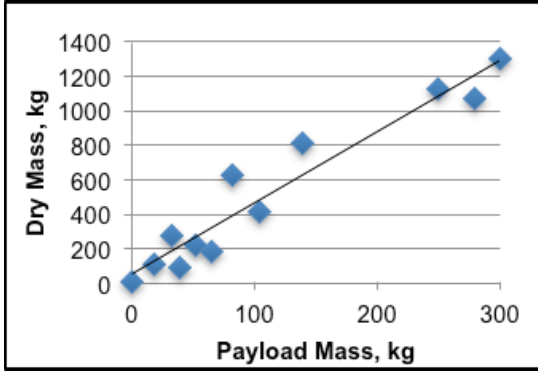


Figure 2. Earth/Lunar Mission Dry Mass.

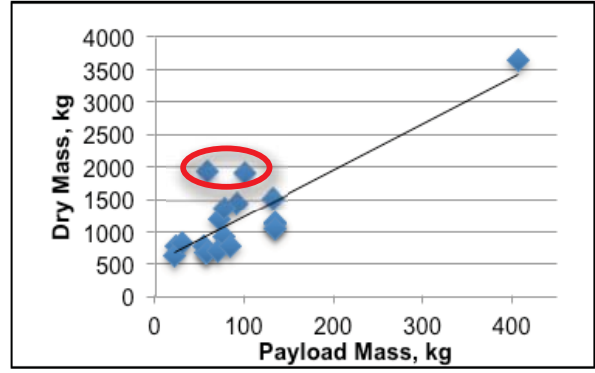


Figure 3. Interplanetary Mission Dry Mass.

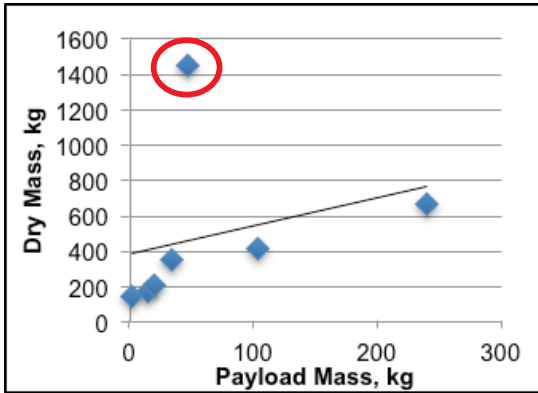


Figure 4. Lander Mission Dry Mass.

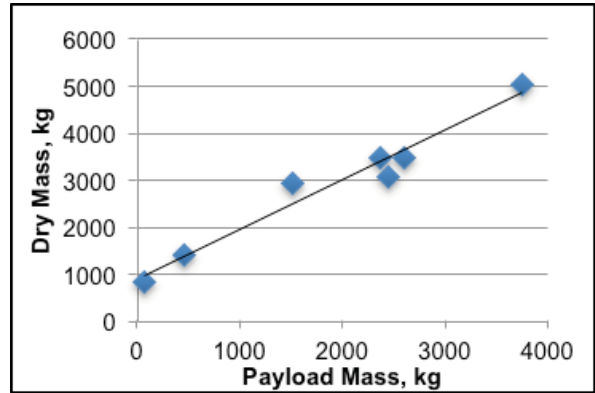


Figure 5. Transfer Vehicle Dry Mass.

However, two of the figures also display some outlying data points. For the interplanetary missions, the two higher-than-expected data points are the two spacecraft which used nuclear fission as a power source, one which was designed to orbit Chiron, and one which was a mission to the Kuiper belt. While on average, the power system for interplanetary spacecraft has 4 times more mass than the payload, the nuclear fission systems are about 20 times heavier than their respective payloads, accounting for the higher dry mass. For the landing vehicles, the outlier is the Advanced Lithium-Ion Venus Explorer (ALIVE), the only Venus lander that has been designed. Because COMPASS had to design Venus vehicles to survive for a long period of time in “high temperature (450° C) and pressure (90 bar)”<sup>9</sup>, the thermal system required to handle the environment involved significant additional mass. While for all spacecraft, the thermal mass is on average smaller than the payload mass and makes up 10% of the spacecraft bus mass, for ALIVE, it is almost 9 times larger than the payload and makes up over 35% of the bus mass. This is the highest thermal-to-payload ratio and second-highest thermal system percentage of all designs completed by COMPASS. The only other design to display similarly high values (the second-highest and highest, respectively) is a rover that was also designed for long life on Venus’ surface, confirming that the additional environmental demands are the cause of the higher dry mass.

With these outliers removed, a linear regression fit was performed on the set of data points for each spacecraft type. The relationships between payload mass and spacecraft dry mass for Earth/lunar missions, interplanetary missions, landers, and transfer vehicles are listed below as Eqs. 1, 2, 3, and 4, respectively.

$$M_D = 4.14 \cdot M_{PL} + 54.66 \quad (1)$$

$$M_D = 7.49 \cdot M_{PL} + 372.71 \quad (2)$$

$$M_D = 2.11 \cdot M_{PL} + 181.97 \quad (3)$$

$$M_D = 1.06 \cdot M_{PL} + 908.20 \quad (4)$$

The relationship between stage vehicle payload and dry mass showed approximately a one kilogram increase of dry mass per kilogram increase of payload; this would imply that the spacecraft bus mass remained nearly constant. With that assumption, and with the knowledge that stage vehicle payloads are not integrated into the spacecraft, but rather separated once they reach their final location, it is possible that the stage mass was not correlated to the payload mass. Instead, COMPASS may have used similarly sized stage busses, and the 908.2 kg in Eq. 4 represents the average of those values. Indeed, a calculation of the correlation between stage payload and stage bus mass gave 0.27, showing little correlation, although a separate calculation for the manned stage vehicles gave a correlation of 0.71. It is likely that more study, with additional data points, is needed to come to a definitive conclusion.

For Earth-orbit missions, on average, the dry mass is equivalent to 4.78 times the payload mass, which agrees with Wertz and Larson’s claim that dry mass ranges from 2 to 7 times payload mass for Earth-orbit satellites<sup>1</sup>, as well as Brown’s estimate that Earth-orbiting spacecraft had an average dry mass to payload mass ratio of 4.8.<sup>5</sup> Brown’s assertion that interplanetary missions averaged 7.5 times the payload mass<sup>5</sup> matches the limit of Eq. 2 for massive payloads. However, we found that on average the interplanetary missions are 12.77 times the payload mass, while landers demonstrated an average of 8.25 times the payload mass. The higher factor of 12.77 can be attributed to a larger portion of COMPASS designs using electric propulsion than Brown’s historical database. This difference will be discussed in the following sections.

### III. Wet Mass

Once the dry mass of the spacecraft is known, it becomes a theoretically calculable matter to determine the overall mass of the spacecraft based on the required velocity changes, or  $\Delta V$ , that will occur during the mission. Assuming that all of the propellant is used by the spacecraft, the ratio of the wet mass to dry mass is given by the rocket equation developed by Tsiolkovsky<sup>2</sup>, given in Eq. 5.

$$M_0/M_f = \exp[\Delta V/(g_0 \cdot I_{sp})] \quad (5)$$

Here, the dry mass is equivalent to the spacecraft’s final mass after the propellant has been used,  $M_f$ , while the wet mass is equivalent to the fully-fueled initial mass,  $M_0$ . The specific impulse ( $I_{sp}$ ) is a characteristic feature of the efficiency of the propulsion system used on the spacecraft; as can be seen in the equation, higher specific impulses require less propellant to achieve the same amount of  $\Delta V$ .

The specific impulses used in COMPASS missions generally fell into three ranges, which corresponded to three different propulsion types; chemical rocket engines, Hall thrusters, and gridded ion engines. The chemical propulsion systems used in design studies include monopropellant, bipropellant, and solid propellant engines, and ranged from 222 to 448 seconds of specific impulse. Both the Hall thrusters and gridded ion engines are types of electric propulsion. Both Ion and Hall thrusters have been used since the 1970s and have included spacecraft like Japan’s Hayabusa.<sup>12</sup> In general, ion thrusters provide higher specific impulses than Hall thrusters; among COMPASS designs, the specific impulse of Hall thrusters ranged from 1,300 to 3,000 seconds, while the ion thrusters ranged from 3,159 to 5,000 seconds.

In order to see how the COMPASS missions corresponded to the theoretical relationship, we compared the wet-to-mass ratio to  $\Delta V$  for applicable system designs. This still excludes non-spacecraft systems such as rovers and balloon gondolas which did not have traditional propulsion methods. In addition, missions where the assumption that the initial mass of the system is equivalent to the dry mass of the spacecraft no longer holds true, containing the sample return missions and an SEP tug

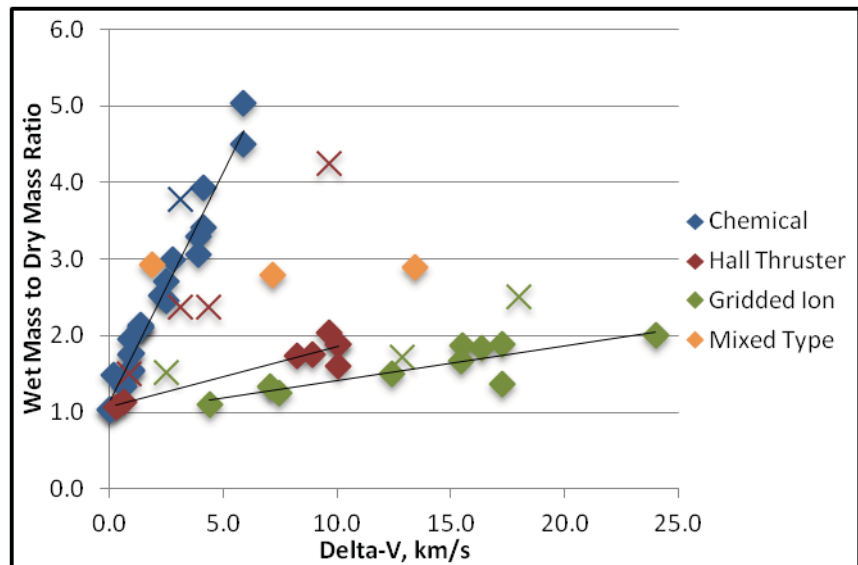


Figure 6. Wet-to-Dry Ratio by Propulsion Type.

designed to move a satellite to a new orbit, were analyzed separately. However, unlike with the dry mass, manned spacecraft and stages were compared to the primary spacecraft missions, since their  $\Delta V$  and wet-to-dry mass ratio are on the same order of magnitude as other missions. That mass ratio is plotted against the  $\Delta V$ , expressed in kilometers per second, in Fig. 6, with each of the propulsion types associated with a different color. The sample return missions were also graphed according to each color, with x-shaped data points representing each spacecraft.

Although the range of data points is broad, there are some notable characteristics. The points appear to radiate out from no  $\Delta V$  and a wet-to-dry mass ratio equal to one, which would be expected given any value of specific impulse in the rocket equation. It is clear that missions requiring higher  $\Delta V$  require higher Isps – with the higher Isp Ion providing almost twice the  $\Delta V$  of the Hall. The electric propulsion missions are not ‘staged’ and thus never have a wet/dry mass ratio greater than 2 (e.g. electric propellant masses are never much greater than the dry spacecraft.) The chemical missions on the other hand show vehicles that have more propellant than dry mass (up to 4 times); many of these designs are staged, some with several. Also, despite obeying an exponential relationship theoretically, the wet-to-dry ratio appears to display a linear dependency on the  $\Delta V$  for each propulsion type, which was added to Fig. 6. Treating this as a linear relationship presents several benefits. First, the Tsiolkovsky rocket equation requires a knowledge of the  $I_{sp}$ , which may not have been specifically determined at the beginning of the study. Furthermore, this method also allows us to account for tendencies within COMPASS design studies. Propellant in excess of the expected required amount is added to vehicle designs, to allow for “an extended mission, or desirable, unplanned maneuvers.”<sup>6</sup> In addition, there is a tendency to utilize thrusters with higher specific impulses for higher levels of  $\Delta V$ , with a correlation of 0.723 on average between the two variables within each propulsion type. This leads to a flatter curve based on the theoretical equation, which can be better matched by the linear approximation.

In addition, there are three data points labeled as "mixed type" propulsion systems. These are three manned missions; two are part of the Human Exploration using Real-time Robotic Operations (HERRO) architecture [citation], which used a nuclear thermal engine with a specific impulse of 900 seconds, while the other was a mission to Mars with a combination of solar electric and chemical propulsion. The leftmost data point was the HERRO crew vehicle sent to Venus, while the rightmost was the crew vehicle sent to Mars. This is a good example of how carrying more propellant than necessary can lead to a greater than expected wet-to-dry mass ratio. The vehicles, being based on the same design, have similar wet and dry masses, despite the Venus mission having significantly fewer  $\Delta V$  requirements.

Since the wet mass is equivalent to the dry mass plus the propellant mass,  $M_{pp}$ , the wet-to-dry mass ratio can be expressed as Eq. 6, below:

$$M_0/M_f = (M_d + M_{pp})/M_d = 1 + M_{pp}/M_d \quad (6)$$

This equation is useful for expressing the linear dependency on  $\Delta V$ . We calculated the linear relationship between the wet-to-dry mass and  $\Delta V$  after setting the y-intercept to 1 for each propulsion type. For the chemical propulsion, the wet-to-dry ratio increases by 0.639 per km/s, for the Hall thrusters, it increases by 0.086 per km/s, and for gridded ion propulsion, it increases by 0.043 per km/s.

As can be seen on the graph, the sample return missions have higher wet mass ratios on average. These range from 1.11 to 2.32 times larger than the expected wet-to-dry mass ratio for each given propulsion type. That largest discrepancy is the FETCH asteroid retrieval mission, which planned to capture an asteroid approximately 500,000 kg in size, which is significantly larger than any sample return mission in history<sup>11</sup>. This indicates that a relationship between the mass that is returned and the increase in the wet-to-mass ratio is likely, but it is not possible to establish at this time due to a lack of available data. Using the established relationships for the major propulsion types and an average of 1.56 times greater ratio for sample return missions, the wet mass for all COMPASS designs can be estimated.

#### IV. Subsystem Breakdown

In addition to using the dry mass to estimate the wet mass, average subsystem breakdowns can be established to estimate the mass of each major component of the spacecraft.<sup>4</sup> With the payload mass already known, we decided to look at the breakdowns for each subsystem as a percentage of the spacecraft dry bus mass. For the applicable satellites, communication payloads were again considered to be a part of the subsystem and the dry bus mass instead of as a payload. We found that in general, the breakdown depended on the type of propulsion, as shown in Table 1.

The EP missions allotted significantly higher percentages to the power and propulsion subsystems, while chemical missions had higher percentages for the guidance, navigation, and control (GN&C), command and data

**Table 1. Subsystem Percent of Spacecraft Bus Mass.**

<b>Propulsion Type</b>	<b>GN&amp;C</b>	<b>C&amp;DH</b>	<b>Comm.</b>	<b>Power</b>	<b>Thermal</b>	<b>Structures</b>	<b>Propulsion</b>
<b>Electric Propulsion</b>	4.7%	5.4%	5.0%	28.0%	8.3%	21.4%	27.1%
<b>Chemical</b>	8.1%	9.1%	13.2%	18.2%	9.1%	24.2%	18.4%

handling (C&DH), and communications subsystems. This was likely attributable to the additional complexity of ion thrusting propulsion systems, as well as the additional power requirements for large EP systems. On average, the maximum power required by spacecraft propelled only by chemical rockets was 0.78 kilowatts (kW), with a maximum of 1.70 kW. On the other hand, EP missions averaged power requirements of 8.50 kW, reaching over 40 kW on the FETCH asteroid retrieval mission, mostly used to power four 10 kW Hall thrusters.<sup>11</sup> This includes only the unmanned spacecraft; piloted vehicles and manned stages using electric propulsion could display power requirements of an entire order of magnitude higher.

In addition to typical electrical propulsion missions, there were two categories of outlying cases to the mass breakdowns: the electric propulsion stages, and the nuclear electric propulsion vehicles. The average breakdown percentages for these two groups are shown in Table 2.

**Table 2. Spacecraft Bus Mass Breakdown for Outlying EP Mission Types.**

<b>Propulsion Type</b>	<b>GN&amp;C</b>	<b>C&amp;DH</b>	<b>Comm.</b>	<b>Power</b>	<b>Thermal</b>	<b>Structures</b>	<b>Propulsion</b>
<b>Stage Vehicles</b>	1.7%	2.2%	1.4%	40.3%	8.3%	18.1%	27.9%
<b>Nuclear EP</b>	1.1%	2.4%	3.1%	73.2%	3.3%	7.2%	9.7%

Both displayed larger percentages in the power subsystems than the average for other electric propulsion missions, and had significantly lower percentages for the GN&C, C&DH, and communications subsystems than the normal missions. The two nuclear-powered missions both had more than half of their bus mass in the power subsystem, because of the radiation shielding, large radiators and other structures associated with the power type, with an associated reduction in every other subsystem. On the other hand, stage vehicles displayed an increase in both the power and propulsion subsystems, with percentages similar to the main electric propulsion missions for the thermal and structure subsystems.

We further used the breakdown on the subsystem level to investigate cost relationships. Using the primary unmanned spacecraft, we calculated the correlation between the mass and cost of each subsystem, and the inflation-adjusted cost per each kilogram of subsystem. These values are listed in Table 3, with the pricing expressed in terms of thousands of dollars, adjusted to federal year 2010 values, per kilogram. As can be seen, all subsystem masses have a significant, positive correlation to the cost, except for the payload. In addition, we found that the power system showed very high levels of correlation, but only once it was broken into solar and radioisotope power systems. Other power types were not common enough among primary unmanned spacecraft types to be analyzed. In general, the payload, guidance, data handling, communication, and radioisotope power subsystems had high cost per mass, ranging between \$593,000 to \$733,000 per kilogram, while the solar power, thermal, structures, and propulsion subsystems tended to be low cost per mass, ranging from \$132,000 to \$203,000 per kilogram.

**Table 3. Subsystem Cost per Kilogram.**

<i>Type</i>	<i>Correlation</i>	<i>Average (\$K/kg)</i>
Payload	-0.235	733
GN&C	0.649	696
C&DH	0.875	663
Comm	0.955	593
Power (Radioisotope)	0.960	736
Power (Solar)	0.946	194
Thermal	0.926	163
Structures	0.888	132
Propulsion	0.926	203

Other power types were not common enough among primary unmanned spacecraft types to be analyzed. In general, the payload, guidance, data handling, communication, and radioisotope power subsystems had high cost per mass, ranging between \$593,000 to \$733,000 per kilogram, while the solar power, thermal, structures, and propulsion subsystems tended to be low cost per mass, ranging from \$132,000 to \$203,000 per kilogram.

## V. Cost

Since mass estimation relationships had already been established, we turned to developing a system-level cost estimation relationship, based on either the bus mass, dry mass, or wet mass. Because the subsystem breakdown showed that the scientific payload mass was uncorrelated payload price, and because there were no costs associated with the propellant, we sought to calculate a price per kilogram of spacecraft bus mass.

As mentioned above, care was taken to convert the reported cost values in each design study to a common time, the Fiscal Year 2010 Constant Dollars (FY10\$), in order to neglect the effects of inflation, which is an important step in developing a cost estimation relationship.<sup>6</sup> 2010 as the normalized fiscal year used for costing; the rates of

inflation for each year were taken from the 2013 NASA index.<sup>14</sup> In addition, the cost used to develop the relationship was the prime cost, which accounts for the development, manufacturing, and integration costs, but not the costs of launch, oversight or the operation of the mission. It should be noted that there are several methods of developing systems (e.g. the amount of test articles varies greatly which significantly impacts cost) so that each spacecraft cost estimate is highly variable and dependent on the design and the assumptions unique to that design.

A graph of the spacecraft prime cost versus the spacecraft bus mass is shown in Fig. 7. As with the dry mass versus payload mass, we only considered the primary spacecraft, which included Earth and lunar missions, interplanetary probes, landers, and stage vehicles. Here, however, the vehicle type had no direct impact on the costing relationship, since mass differences were already accounted for in the earlier equations. It appears that most data points seem to radiate out from the graph's origin, with a few outliers to that pattern. In general, the spacecraft seemed to range from \$200,000 per kg of bus mass, up to \$1,000,000 per kg of bus mass. There were two notable classes of outliers to this range. The two gondola designs cost less than \$10,000 per kg, while the four Mars Ascent Vehicles cost more than \$2,000,000 per kg.

Other costs per kilogram were found to be associated with different mission types, as illuminated by the subsystem breakdowns for both mass and cost. Primarily, the common mission types with different costs were, in order of decreasing cost per kg, radioisotope-powered spacecraft, solar-powered chemical spacecraft, SEP spacecraft, and stage vehicles (all of which were also SEP missions). A graph showing only these missions is found in Fig. 8, with trendlines added to each data set. The average cost per kilogram for each mission type is also listed in Table 4. As described in the subsystem analysis, GN&C, C&DH, communications, and radioisotope power subsystems had higher costs per kilogram, while thermal, structure, propulsion, and solar power subsystems had lower specific costs. The spacecraft cost per kilogram can be seen as an average of each subsystem cost per kilogram, weighted according to the subsystem mass distribution percentage. The largest difference subsystem, in general, as well as the subsystem which showed the greatest difference among different mission types, was the power subsystem, and it therefore had a determining effect on the cost per kilogram of spacecraft bus mass. Since all radioisotope missions had a higher price per power subsystem, they had a higher average prime cost per spacecraft bus mass. The solar-powered craft, on the other hand, had a lower price per power subsystem; therefore, the higher the percentage of dry bus mass was distributed in the power system, the lower the average cost per kg ended up being, which accounts for the stage missions being the cheapest price per kilogram. In addition to these four categories, the four MAV designs, and the two gondola designs, one of the nuclear-powered electric propulsion spacecraft had cost data available. The nuclear electric

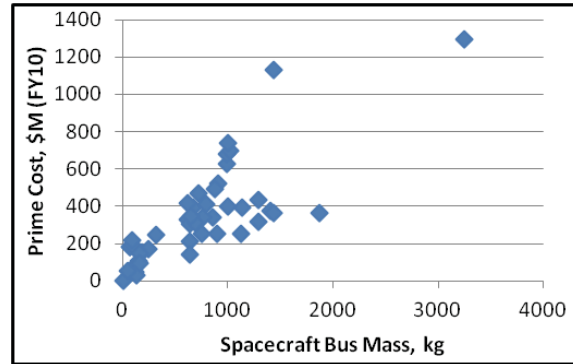


Figure 7. Prime Cost versus Spacecraft Bus Mass.

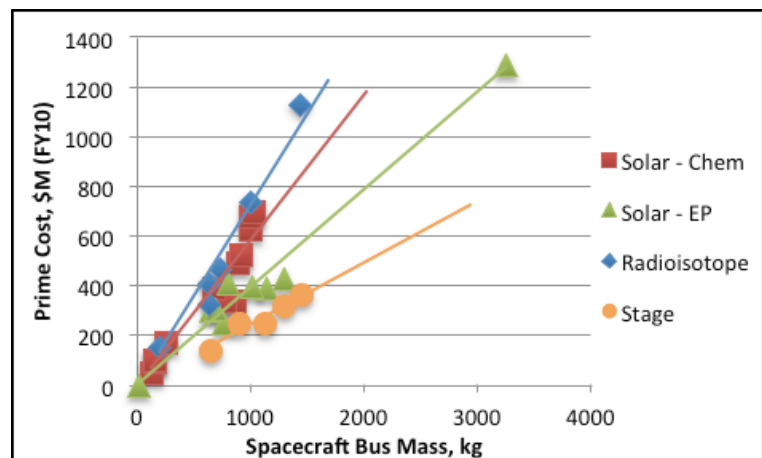


Figure 8. Prime Cost by Power and Propulsion Type.

craft bus mass. The solar-powered craft, on the other hand, had a lower price per power subsystem; therefore, the higher the percentage of dry bus mass was distributed in the power system, the lower the average cost per kg ended up being, which accounts for the stage missions being the cheapest price per kilogram. In addition to these four categories, the four MAV designs, and the two gondola designs, one of the nuclear-powered electric propulsion spacecraft had cost data available. The nuclear electric

Table 4. Cost per Spacecraft Dry Bus Mass.

Mission Type	Average (\$K/kg)	Std. Deviation (\$K/kg)
Radioisotope (n=7)	708	99.8
Solar – Chemical (n=12)	583	109.6
Solar – EP (n=8)	364	67.0
Solar EP Stage (n=5)	238	28.8
MAVs (n=4)	2,488	299.6
Gondolas (n=2)	2.3	N/A
Nuclear – EP (n=1)	193	N/A

propulsion vehicle displayed a lower cost than even the SEP stages, which verifies the correlation between higher power subsystem mass distributions and lower specific costs. The summary of these average costs per spacecraft bus mass, along with the calculated standard deviation, when calculable, were added to Table 4.

## VI. Historical Comparison

In order to see how the mass and cost relationships functioned outside of the COMPASS mission database, we endeavored to compare the models to historical spacecraft missions. Basic cost and mass data, including the payload mass, dry mass, overall mass, and development costs, were recorded for multiple spacecraft. Mass data was taken from NASA's National Space Science Database Center<sup>15</sup> for several spacecraft, while a data set compiled by Butts and Linton<sup>13</sup> was used to record spacecraft development cost data for multiple craft. As before, care was taken to convert all costing data into Federal Year 2010 dollars; the launch year was used as an estimate for this purpose. The missions for which cost data was available included earth and lunar satellites such as QuikSCAT, ACRIMSAT, Cloudsat, Aura, and Terra (all solar-powered, chemical-propelled) while the interplanetary missions included the radioisotope-powered New Horizons, Galileo, and Cassini missions, the solar-powered, chemical spacecraft NEAR Shoemaker, the Mars Climate Orbiter, MESSENGER, the Mars Reconnaissance Orbiter, Juno, and Mars Observer, as well as the SEP missions Hayabusa, Deep Space 1, and Dawn, along with the Mars Pathfinder lander (solar chemical). In addition to these missions, mass data was also available for these Earth and lunar missions: Aquarius, Aqua, ACE, Jason-2, TRMM, EO-1, SORCE, GRACE, Suomi NPP, Artemis, Cluster II, and GOCE. Interplanetary missions with only mass data included Mariner 9 and 10, Voyager 1, and Deep Impact, while the Huygens lander, Deep Space 2, Lunar 17, Ranger 7, and Viking 1 made up the landers used for mass data.

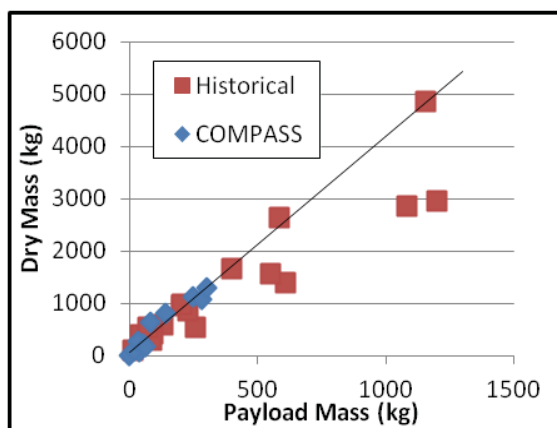


Figure 10. Historical Earth/Lunar Comparison.

Fig. 10 shows the relationship between payload mass and dry mass for the Earth and lunar missions, displaying both the COMPASS design data and the historical missions. Although several historical missions fall close to the trend line among COMPASS spacecraft, which was added to the figure, many are significantly lower than would be predicted, and there is a wider range of variation than seen in the COMPASS designs. These missions ranged from over 200 kg above expected to over 2,000 kg below expected. This discrepancy is due to the fact that the historical data consists of a wide majority of low-Earth orbit missions, while the majority of COMPASS designs were in fact lunar missions. We plan to split the earth and lunar missions out in future analyses.

On the other hand, as shown in Fig. 11, the historical interplanetary missions ranged from 375.5 kg above to 588.1 kg below expected, and on average were 200.0 kg below the trend displayed by the COMPASS missions. The large discrepancy between the COMPASS and historical interplanetary missions can be explained by COMPASS' tendency to use electric propulsion more commonly than

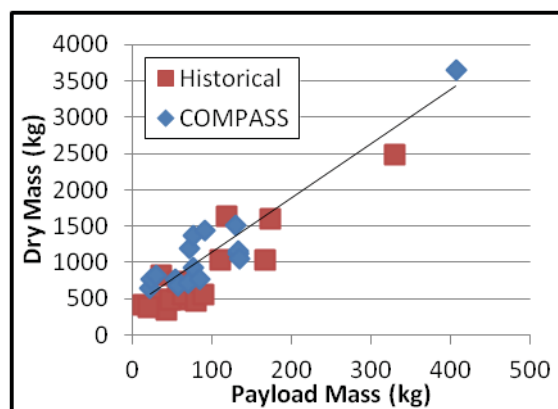


Figure 11. Historical Interplanetary Comparison.

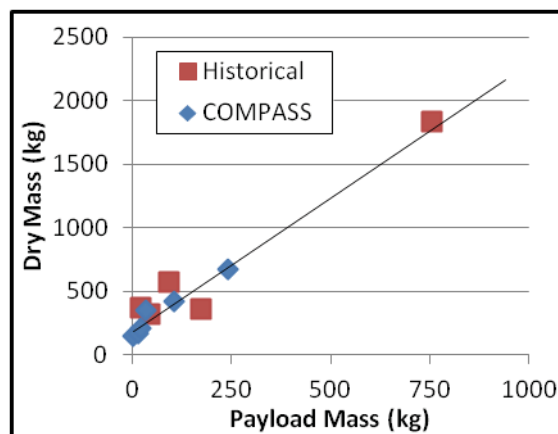


Figure 12. Historical Lander Comparison.



chemical propulsion. The mass subsystem breakdowns and the historical comparisons both confirm that EP missions require greater amounts of dry mass (large power systems in lieu of chemical propellant so dry masses are higher); this was not explored previously because of the small number of comparable COMPASS missions; only 3 out of 18 unique interplanetary designs used chemical propulsion. On the contrary, only 3 out of 16 historical missions with available data used electric propulsion. On average, COMPASS electric propulsion missions had 18.3 times the dry mass of the payload, while historical EP had 24.5 times the dry mass. On the other hand, chemical propulsion COMPASS missions had a dry mass 9.1 times larger than the payload on average, with historical missions demonstrating an increased factor of 9.4. While this might make chemical missions sound more advantageous (lower dry mass) the truth is that electric and chemical propulsion enable completely different missions; chemical propulsion is limited to  $\sim 2$  km/s  $\Delta V$  (without staging) while electric propulsion can provide an order of magnitude more  $\Delta V$ . This difference allows, for example, electric propulsion to rendezvous with two asteroids (aka the Dawn mission) which would only be a single flyby with a chemical mission. It is our intent to break out electric propulsion and chemical missions and develop separate models in the future.

The landers, shown in Fig. 12, displayed the closest adherence to the expected values, averaging only 14.5 kg higher than predicted, but they also included the fewest missions. Further data could be used to validate whether this relationship is accurate.

After this analysis was completed, the historical missions were reorganized based on power and propulsion types, and the average cost per kilogram of spacecraft bus mass was calculated, using the cost categories previously developed. However, there were no gondola, nuclear-powered, ascent vehicles, or rocket stages with which to take averages. Averages and standard deviations were calculated for the three main categories (radioisotope, solar chemical, and SEP spacecraft), and listed in Table 5. As before, the radioisotope missions were the most expensive, followed by the solar chemical, with the SEP being the cheapest. The disparity between the historical radioisotope and the COMPASS radioisotope average costs ( $\sim \$1,000K/kg$  and  $\sim \$700K/kg$ , respectively) may be due to the fact that COMPASS designs usually assume the radioisotope systems are government furnished and not included in the cost. Further investigation is needed to test this premise. Both the SEP and chemical historical missions were within a standard deviation of the previously calculated COMPASS price per bus mass, which provides some substantiation to COMPASS cost products.

**Table 5. Cost per Historical Spacecraft Bus Mass.**

<i>Mission Type</i>	<i>Average (\$K/kg)</i>	<i>Std. Deviation (\$K/kg)</i>
Radioisotope	1,048	93.3
Solar – Chemical	614	218.2
Solar – EP	359	43.2

## VII. Conclusion

In this paper, we have developed a parametric estimation model for both spacecraft mass and cost based on previous COMPASS designs. We found the dry mass to be dependent on the payload mass, with the specific relationship varying based on the mission type, and we confirmed the principle of these relationships to be correct given historical mission data, although more variance was seen. Furthermore, we developed a method for determining propellant and total spacecraft wet mass based on linear relationships of  $\Delta V$ , rather than through the rocket equation, which we hope to be more useful for COMPASS design studies. We found, as expected, electric and chemically propelled spacecraft have notably different dry mass and costs trends. Finally, we found that spacecraft development costs were most closely related to the spacecraft bus mass, which excludes the propellant and payload masses. This cost per kilogram was calculated for different propulsion and power system types, along with uncommon design types. Radioisotope powered spacecraft were found to be more expensive per kilogram than solar powered craft, which was confirmed by historical data. We hope this work will aid in preliminary scoping of future COMPASS design studies, as well as inspiring future work in early design process system-level estimation relationships.

## Acknowledgments

Matthew W. Gerberich thanks the Lewis' Educational and Research Collaborative Internship Project for his opportunity to work on this model for the past three summers, and both authors thank all members of the COMPASS team for their continued dedication and hard work, and in particular Melissa McGuire for her leadership and assistance on this research.

## References

- <sup>1</sup>Larson, W. J., and Wertz, J. R., *Space Mission Analysis and Design*, 3<sup>rd</sup> ed., Microcosm Press, El Segundo, CA, and Springer, New York, 1999, pp. 312.
- <sup>2</sup>Ibid, p. 690.
- <sup>3</sup>Ibid, pp. 797-799.
- <sup>4</sup>Ibid, pp. 894-896.
- <sup>5</sup>Brown, C. D., *Elements of Spacecraft Design*, edited by J.S. Przemieniecki, AIAA, Reston, VA, 2002, pp. 21-24.
- <sup>6</sup>Ibid, p. 36.
- <sup>7</sup>McGuire, M. L., Oleson, S. R., and Sarver-Verhey, T. R., "Concurrent Mission and Systems Design at NASA Glenn Research Center: The Origins of the COMPASS Team," NASA TM-2012-217283, AIAA-2011-06396, 2012.
- <sup>8</sup>Oleson, S. R., and McGuire, M. L., "COMPASS Final Report: Lunar Relay Satellite," NASA TM-2012-217140, 2012.
- <sup>9</sup>Landis, G. A., Dyson, R., McGuire, M. L., Oleson, S. R., Schmidt, G. R., and Grantier, J., et al., "Human Telerobotic Exploration of Venus: A Flexible Path Design Study," *2010 Joint Propulsion Conference*, Nashville, TN, AIAA, 2011.
- <sup>10</sup>Dankanich, J. W., and Klein, E., "Mars Ascent Vehicle Development Status," *IEEE Aerospace Conference*, Big Sky, MT, 2012.
- <sup>11</sup>Brophy, J. R., Friedman, L., and Culick, F., "Asteroid Retrieval Feasibility," *IEEE Conference Proceedings*, 2012.
- <sup>12</sup>Goebel, D. M., and Katz, I., *Fundamentals of Electric Propulsion: Ion and Hall Thrusters*, John Wiley and Sons, Hoboken, NJ, 2008, pp. 2-6.
- <sup>13</sup>Butts, G., and Linton, K., "The Joint Confidence Level Paradox: A History of Denial," *NASA Cost Symposium 2009*, Denver, CO, 2009, pp. 98-109.
- <sup>14</sup>Hunt, C., "2012 NASA New Start Inflation Index use in FY13," *NASA Cost Analysis Division* [online database]. URL: [http://www.nasa.gov/pdf/601957main\\_2011%20NASA%20New%20Start%20Inflation%20Index%20use%20in%20FY12.pdf](http://www.nasa.gov/pdf/601957main_2011%20NASA%20New%20Start%20Inflation%20Index%20use%20in%20FY12.pdf) [cited 15 July 2013].
- <sup>15</sup>Grayzeck, E., and Bell, II, E. V., "NSSDC Master Catalog", *National Space Science Data Center* [online database], <http://nssdc.gsfc.nasa.gov/nmc/> [cited 20 July 2013].